International Journal of Precision Engineering and Manufacturing (2024) 25:487–496
https://doi.org/10.1007/s12541-023-00866-9

Online ISSN 2005-4602
Print ISSN 2234-7593

REVIEW

Recent Developments in Finite Element Analysis of the Lumbar Spine

Batbayar Khuyagbaatar[1] · Kyungsoo Kim[2] · Yoon Hyuk Kim[3,4]

Received: 19 April 2023 / Revised: 26 July 2023 / Accepted: 27 July 2023 / Published online: 10 August 2023

Abstract

Finite element (FE) modeling is widely used to study the biomechanical effect of material properties, surgical procedures, and loading and boundary conditions on the lumbar spine. Since several studies have presented FE analyses of the lumbar spine in relation to spine biomechanics, soft tissue modeling, intervertebral discs, facet joints, load-sharing behaviors of lumbar motion segments, and FE modeling methods, detailed analyses of disc degeneration or muscle force prediction have been little considered. This study focused on recent developments in FE modeling of the lumbar spine, including disc degeneration, muscle force prediction, and clinical applications. Modeling and analysis from the bone to soft tissue and muscle forces, as well as the validation and application of these models were provided and discussed with material properties, element types, loading and boundaries, geometric parameters, and muscle force modeling. Experimental data was summarized for validation of the FE model. Application studies were briefly reviewed, in which the majority of FE models focused on spinal degeneration diseases and surgical instrumentation techniques. Although muscle force prediction and optimization are challenging with FE modeling due to their complexity and redundancy, several studies have predicted muscle activation and spinal forces for injury prevention assessments and treatment strategies. The level of modeling prediction and representation can be improved with subject-specific data, and integration of FE and musculoskeletal models could generate a comprehensive analysis of the lumbar spine in clinical applications.

Keywords Lumbar spine · Disc degeneration · Muscle force · Clinical application · Finite element model

1 Introduction

Finite element (FE) modeling is widely used in spine biomechanics research because it evaluates stresses and strains in bony and soft tissue structures more realistically [1]. Single functional spinal units (FSUs) [2–4], as well as L3–L5 [5, 6], L2–L4 [7], L1–L3 [8], L2–L5 [9], and L1–L5 [10–14] spinal levels have been modeled to study the biomechanical effect of material properties, surgical procedures, and loading and boundary conditions on the lumbar spine, where small segments or FSUs are often used to evaluate the effect of different types of surgical interventions [11]. Xu et al. [7] analyzed stress concentrations of fixation rods with different fixation methods using a two-level model, while Ambati et al. [6] compared the stability of different fusion constructs using an L3–L5 lumbar FSU instrument with interbody fusion cages. In addition, the sacrum to lumbar spine region has been included in multi-segment spine models with consideration of global parameters such as pelvic incidence and lordosis, which are of great interest to clinicians [15–23]. Haddas et al. [16] first modeled scoliotic lumbosacral spines in relation to the Cobb angle based on in vivo computed tomography (CT) scans of patients. Furthermore, Park et al. [22] investigated the effects of single-level degeneration on whole lumbosacral spine biomechanics. In parallel with these studies, several subject-specific detailed models have been developed [17, 24–26], such as that of Haj-Ali et al.

This paper is an invited paper (Invited Review)

Yoon Hyuk Kim
yoonhkim@khu.ac.kr

[1] Biomechanical Research Laboratory, Department of Technical Mechanics, Mongolian University of Science and Technology, Ulaanbaatar, Mongolia

[2] Department of Applied Mathematics, Kyung Hee University, Yongin, Korea

[3] Department of Mechanical Engineering, Kyung Hee University, 1732, Deogyeong-daero, Giheung-gu, Yongin-si 17104, Gyeonggi-do, Korea

[4] Integrated Education Institute for Frontier Science and Technology (BK21 Four), Kyung Hee University, Yongin, Korea

[17], who generated an L1–S1 model using patient-specific CT scans to simulate the spondylolysis effect on lumbar segments. Recently, FE models have been combined with musculoskeletal representations to conduct comprehensive and realistic biomechanical analyses [27–33].

Several studies have presented FE analyses of the lumbar spine in relation to spine biomechanics [34], soft tissue modeling [35], intervertebral discs [36], facet joints [37], load-sharing behaviors of lumbar motion segments [38], and FE modeling methods [39–45]. Schmidt et al. [36] reviewed an FE simulation of lumbar intervertebral discs (IVDs) with a focus on functional biomechanics, while Mengoni [37] provided a systematic review of FE modeling of the facet joints. In addition, Ghezelbash et al. [38] discussed the relevant findings of in vitro and FE modeling studies of lumbar motion segments, specifically with regard to the load-sharing contributions of spinal tissues in both normal and perturbed conditions. Recently, Knapik et al. [43] systematically reviewed computational modeling methodologies of the lumbar spine and identified that musculoskeletal models are capable of evaluating whole-body motion and deformations with kinematics-driven data, whereas the FE model enables a detailed investigation into individual tissue deformations and stresses [43]. Furthermore, Dreischarf et al. [46] compared eight well-established FE models of the lumbar spine to in vitro and in vivo measurements in terms of intervertebral rotations, intradiscal pressure (IDP), and facet joint force (FJF) under pure moments and combined loadings to show the validity of FE analysis. Despite the depth of these reports, detailed analyses of disc degeneration or muscle force prediction have been little considered. This study focuses on recent developments in FE modeling of the lumbar spine, including disc degeneration, muscle force prediction, and clinical applications. Articles were searched through the PubMed and Science Direct databases between 2013 and 2023 with the following keywords: 'lumbar', 'spine', 'muscle', 'disc generation', 'finite element', and 'model'. The inclusion criteria were language in 'English' and a study population of 'humans.' Several older significant and relevant studies were also included.

2 FE Modeling Methodologies

The FE model including bony structures, IVDs, ligaments, and facet cartilages in flexion, extension, lateral bending, and axial rotation was depicted in Fig. 1. The details for FE modeling details including material properties were summarized in Table 1.

2.1 Bony Structures

Cancellous and cortical bones, as well as post-bone material, are generally included in FE models. Computed tomography (CT) imaging is frequently used for generating spinal bony parts, although CT-based modeling requires substantial manual intervention for segmentation, threshold, and region-growing [1, 43]. Some studies have utilized radiographs [47] and geometric parameters [48]. Nikkhoo et al. [47] used lateral and anterior–posterior X-Ray images to develop an FE model of L1–S1 that automatically updated the spinal geometry of patients based on independent parameters. Bashkuev et al. [48] developed a parametric model of the L4–L5 motion segment considering natural variations in spinal geometry using 40 different parameters. In addition, several modeling techniques have been proposed, including an automated landmark identification method for subject-specific FE modeling of the lumbar spine that identifies all necessary landmarks for model creation using CT geometry of a spinal bone [49]. A parametric computer-aided design

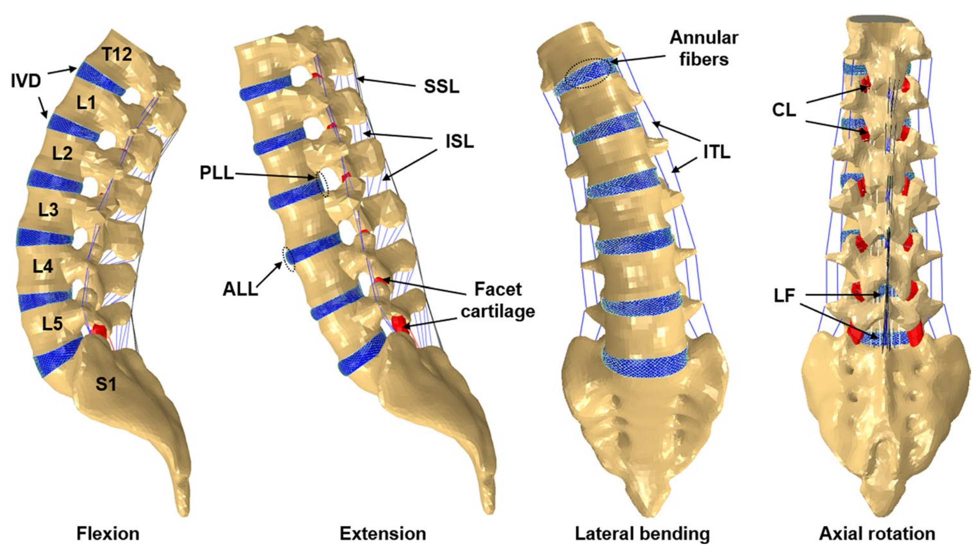

Fig. 1 FE model of the lumbar spine including bony structures, IVDs, ligaments, and facet cartilages in flexion, extension, lateral bending, and axial rotation (IVD—intervertebral disc; ALL—anterior longitudinal ligaments; PLL—posterior longitudinal ligament; ISL—interspinal ligament; SSL—supraspinal ligament; CL—capsular ligaments; LF—ligament flavum)

Table 1 FE modeling details including material properties

	Zhang et al. [21]	Park et al. [22]	Xu et al. [25]	Nikkhoo et al. [47]	Umale et al. [51]	Spina et al. [62]	Ellingson et al. [79]
Modeling levels	L1–S1	L1–S1	L1–L5	L1–S1	T12–S1	L1–L5	L3–S1
Bone geometry	CT	CT	CT	Parametric-simplified	CT and mapping block technique	CT	CT
Cortical bone	E = 10,000 MPa v = 0.30	E = 12,000 MPa v = 0.30	E = 12,000 MPa v = 0.30	E = 12,000 MPa v = 0.30	E = 12,000 MPa v = 0.30	Orthotropic elastic E_1 = 8000 MPa v_{12} = 0.40 E_2 = 8000 MPa v_{23} = 0.30 E_3 = 12,000 MPa v_{31} = 0.35	E = 12,000 MPa v = 0.30
Cancellous bone	E_{11} = 140 MPa, v_{12} = 0.45 E_{22} = 140 MPa, v_{13} = 0.31 E_{33} = 140 MPa, v_{23} = 0.21	E = 100 MPa v = 0.20	E = 100 MPa v = 0.20	E = 200 MPa v = 0.25	E = 100 MPa v = 0.20	Neo-Hookean E = 100 MPa v = 0.20	E = 100 MPa v = 0.20
Posterior bone	E = 3500 MPa v = 0.30	E = 3500 MPa v = 0.25	E = 3500 MPa v = 0.25	–	E = 3500 MPa v = 0.25	Neo-Hookean E = 3500 MPa v = 0.30	E = 3500 MPa v = 0.25
Cartilaginous endplate	E = 23.80 MPa v = 0.40	E = 23.80 MPa v = 0.40	E = 23.80 MPa v = 0.40	E = 23.80 MPa v = 0.25	–	Neo-Hookean E = 23.80 MPa v = 0.42–0.45	E = 5 MPa v = 0.17
Facet cartilage	Frictionless contact Neo-Hookean C_{10} = 2 D = 0.3	Frictionless contact E = 11 MPa v = 0.4	Frictionless contact	Frictionless contact	Facet fluid: Viscoelastic C_0 = 17.8 kPa C_1 = 7.1 kPa β = 1.0/s k = 1720 MPa	Frictionless contact E = 30 MPa v = 0.4	Frictionless contact
Nucleus	Mooney–Rivlin C_1 = 0.12 C_2 = 0.03 D = 0.3	Incompressible fluid filled cavity	Mooney–Rivlin C_1 = 0.12 C_2 = 0.09	Mooney–Rivlin C_1 = 0.12 C_2 = 0.03	Viscoelastic C_0 = 17.8 kPa C_1 = 7.1 kPa β = 1.0/s k = 1720 MPa	Neo-Hookean E = 1 MPa v = 0.49	E = 1 MPa v = 0.49
Annulus ground	Yeoh C_{10} = 0.0146 C_{20} = − 0.0189 C_{30} = 0.041 D = 0.3	Mooney–Rivlin C_1 = 0.18 C_2 = 0.045	Mooney–Rivlin C_1 = 0.56 C_2 = 0.14	Mooney–Rivlin C_1 = 0.18 C_2 = 0.045	Hill foam C_1 = 0.115 b_1 = 4 C_2 = 2.101 b_2 = − 1 C_3 = − 0.893 b_3 = − 2	Holmes–Mow E = 1 MPa v = 0.40	Neo-Hookean C_{10} = 0.25 D_1 = 0.78
Annulus fibers	Nonlinear elastic	Hyperelastic	Nonlinear elastic	Nonlinear elastic	Orthotropic nonlinear elastic	Fiber-exponential-power β = 3.5 α = 65 β = 2.0 ξ = 0.296	Nonlinear elastic
Ligaments	Nonlinear elastic	Hyperelastic	Nonlinear elastic	Nonlinear elastic	Orthotropic nonlinear elastic	Nonlinear elastic	Nonlinear hypoelastic

(CAD) model was used to generate a parametric FE model of the lumbar spine that integrated independent tuning of morphometrical parameters [50], and the mapping block technique was applied to model T12–S1, which allowed for a continuous mesh model from the superior to inferior vertebrae [51]. Lalonde et al. [52] developed a free-form deformation technique to deform a detailed FE mesh of the spine to subject-specific geometry. It should be noted that meshing elements affect the accuracy of the model, and hexahedral meshing is usually recommended for solid components because it is computationally efficient and has better numerical stability than tetrahedral meshing [50, 51]. Generally, bony components have been modeled with elastic material properties [46].

2.2 IVDs, Ligaments, and Facet Joints

The IVD is important for the regulation of flexion responses, whereas capsular ligaments (CL), anterior longitudinal ligaments (ALL), and discs are more dominant under extension [39]. The posterior longitudinal ligament (PLL), ligament flavum (LF), interspinal ligament (ISL), and supraspinal ligament (SSL) are generally resistant to flexion [53], while intertransverse ligaments (ITL) mainly contribute to the lateral bending stiffness of the motion segment [2], and facet joints allow greater flexion, extension, and lateral bending movements but resist rotation [54]. Naserkhaki et al. [3] reported that ligaments resist 45–75% of flexion, whereas facet joints and discs resist 20–33% and 48–60% of the extension movement, respectively.

The IVD consists of the annulus fibrous containing ground substances and fibers, as well as the nucleus pulposus and endplates. Recent studies have used hexahedral elements with Mooney–Rivlin [22], neo-Hookean [55], and Yeoh [21] hyperelastic materials as annulus ground substances, while the nucleus pulposus, which represents approximately 44% of the surface of the disc, was modeled with fluid elements [22] or Mooney–Rivlin hyperelastic material [56–58]. Truss elements were used to model the fibers of the annulus fibrosus with tension-only material properties [22], as well as shell elements with rebar properties [16]. The fibers which reinforce the ground substance in the radial direction are oriented approximately 30 degrees from the horizontal surface (the bottom portion of the IVD) [59]. The number of fiber layers ranges from 2 to 16 depending on the study [46]. The stiffness of each annular fiber layer is different since external layers have a greater stiffness than their internal counterparts [25]. The endplate was modeled to an approximate 0.5–0.6 mm thickness with solid elements by extruding the surface of the vertebral body [6, 14, 58].

The ligaments were modeled using truss [60], spring [61], shell [16], connector [49], and solid [54] elements. During the creation of the FE model, ligament attachment points were manually defined using anatomical landmarks. Subsequently, the automatic modeling technique was developed for determining the attachment points of ligaments [49]. The lack of experimental data mandated the use of major assumptions regarding the material properties of the ligaments which were simulated with linear, bilinear, and nonlinear force–displacement and stress–strain properties [3].

Facet joints are among the most difficult elements to model and are distinguished by a uniform gap between the articulating surfaces [43]. Facet cartilages have often been modeled on the superior and inferior plane of the facet joints with isotropic linear elastic wedge elements since the actual location and thickness of the cartilage cannot be determined from a CT scan [22, 49]. Frictionless surface-to-surface soft contact and an initial gap of 0.1–0.5 mm were assumed to exist between cartilages [22, 62], and a friction coefficient of 0.1 was used for the contact of facet joints [57].

2.3 Muscle Force Modeling

An individual muscle in the lumbar region was represented in a model as a straight line between its origin and insertion to define the muscle force direction [63]. The origins and insertions were obtained from the literature and adapted to the FE model based on anatomical landmarks of bony structures [64]. Physiological cross-sectional areas (PCSAs) of the muscles were obtained from the literature to calculate muscle stress [65]. Recent FE models have included a large number of muscles [63–66]. Kim et al. [64] considered 58 pairs of superficial muscles: longissimus pars lumborum (5), iliocostalis pars lumborum (4), longissimus pars thoracis (12), iliocostalis pars thoracis (8), psoas (11), quadratus lumborum (5), external oblique (6), internal oblique (6), and rectus abdominus (1); and 59 pairs of deep muscles: thoracic multifidus (12), lumbar multifidus (20), interspinales (6), intertransversarii (10), and rotatores (11). El Ouaaid et al. [66] used a kinematics-driven thoracolumbar FE model consisting of 46 local and 10 global muscle fascicles to estimate muscle forces, spinal loads, and stability during elevations with an optimization algorithm. Muscle forces were then predicted to satisfy the force and moment equilibrium using the calculated net intersegmental forces and moments, ligament forces, and facet joint forces by the conventional optimization technique due to their complexity and redundancy [64–66]. The objective function was normally the summation of cubic muscle stresses and the maximum isometric muscle force was determined as the upper boundary of the individual muscle force.

The concept of the follower load (FL) has been used to assume that resultant muscle forces follow a path through the vertebrae [25, 61, 67]. The FL concept was applied to the lumbar spine FE model to simulate standing and compared with other loading modes [68]. It was indicated that FL delivers the most probable intersegmental rotations and FL of 500 N was suggested for the simulation of a standing position with the lumbar spine model. In addition, Han et al. [69] demonstrated that spinal muscle can create a compressive FL in the lumbar spine during a standing posture, and recommended this approach for experimental and numerical studies. Kim et al. [64] proposed a modified concept of the

FL, whereby the compressive load aimed for a half-radius of the body near the body center, and analyzed muscle coordination and trunk muscle activation using an optimization scenario. Shih et al. [70] compared the effects of concentrated, follower, and muscular loads on lumbar biomechanics during flexion. The results showed that the FL can aid in the avoidance of unreasonably high flexion and anterior shear at the disc level. Moreover, a realistic location for the FL path was studied for the lumbar in a neutral standing position.

3 Clinical Applications

3.1 Model Validation

Models are validated using comparisons with available experimental or computational data, which provides confidence to the model predictions [37, 46]. Most FE models are validated using in vitro range of motion (ROM), FJF, and IDP data with single or combined loadings [14, 53–55, 71] where experimentally observed moment-rotation data are commonly available [46, 67, 72, 73]. Rohlmann et al. [72] measured the ROM of the human lumbar spine under pure moments of 3.75, 7.5, and 7.5 Nm with a follower load of 280 N in vitro and found that at 7.5 Nm the experimentally observed L1–5 ROMs were 24°–37° in flexion–extension, 18°–42° in left–right lateral bending, and 7°–17° in left–right axial rotation [72]. Moreover, models can be validated using FJF [74–76] and IDP [77, 78]. Wilson et al. [75] measured FJFs in cadaver lumbar spines using flexible resistive sensors (Tekscan) under pure moments of 7.5 Nm and reported values of 55–110 N for axial rotation and 10–50 N for extension. In addition, extra-articular strains were applied to measure the FJF during axial rotation (71 ± 25 N), extension (27 ± 35 N), and lateral bending (25 ± 28 N). Wilke et al. [78] measured the IDP in the L4–5 disc in vivo and returned values in flexion, extension, lateral bending, and axial rotation of 1.08, 0.60, 0.59, and 0.70 MPa, respectively.

3.2 Spinal Degeneration Modeling

Spinal degeneration has been the subject of many lumbar spine FE models, whereby various parameters have been altered to understand the role of each structure in spinal biomechanics [79]. Disc degeneration can be predicted with the FE model by determining the locations of the greatest stresses in the endplates and annulus where failures can initiate [80], and numerous studies have modeled the disc degeneration process [9, 22, 48, 79]. Li et al. [9] simulated lumbar decompression surgery for moderated disc degeneration where the disc height was reduced by 40%. Park et al. [22] investigated intersegmental rotation, nucleus pulposus IDP, and FJF under various grades of disc degeneration. Those authors simulated disc degeneration by changing the geometry and material properties based on clinical classifications. Three parameters were used to describe disc degeneration: disc height, compressibility increase, and material property changes of the annulus fibrosis and ligaments. Rohlmann et al. [81] reported that a 20% decrease in disc height can generate mildly degenerated discs with increased nucleus compressibility. Bashkuev et al. [48] used a probabilistic FE model and found that stiffening of the motion segment led to an increase in the disc degeneration process. Disc height has been indicated as the most influential parameter on the mechanical behavior of discs, and reducing the height by only 10% has opposite results to those previously identified [36]. Other studies have investigated spinal degenerative disease models including those of osteoporosis [82] and osteophytes [58]. Kang et al. [82] modeled the osteoporosis bone model with lower bone density and elastic modulus, while the osteophyte formation model was created with disc height losses from 16 to 82% [58]. However, there are few studies on the effects of ligament properties or failures on the lumbar spine [3, 79]. Ellingson et al. [79] investigated the impacts of ligament degeneration on the functional mechanics of the lumbar spine by gradually removing ligaments from the motion segment and reported that incremental ligament failure produced an increased ROM and decreased stiffness in the lumbar spine FE model.

3.3 Surgical Interventions

FE analysis of spine biomechanics can be used to assess scenarios for a range of spinal disorders or associated surgical interventions through the evaluation of tissue deformations and stresses [37, 43]. The majority of studies have simulated the impacts of various surgical procedures as well as designed and assessed new surgical instrumentation on the lumbar spine based on validated intact models. such as screw fixation and fusion cages [6, 7, 13, 60, 83–90], artificial discs [14] cement discoplasty [91], facetectomy [54], laminectomy [9, 62, 92], and osteotomy [93]. Stress concentrations in rods and pedicle screws have been investigated since the material properties and geometry variations in the fixation devices affect spinal biomechanics, which is related to the possible failure of spinal instrumentation such as broken screws and rods. Guo et al. [13] used topology optimization to determine the optimal rod and fixation design to reduce stress in the rods while decreasing pressures and stresses in spinal tissues. In surgical simulation studies, the ROM or instability of the spine segment has been mainly compared among surgical procedures when experimental investigations are difficult or impossible [62]. Furthermore, the FE method has been expanded to the fields of scoliosis [94] and spinal disorder prevention and treatment [20, 95, 96].

In addition, the influence of loading rate and frequency on the lumbar spine has been reported [8, 97].

3.4 Muscle Force Prediction

Recently, muscle force modeling and prediction have been effective for assessments of spinal injury risk and the design of effective prevention and treatment programs because muscles act important role in spine stabilization by generating the substantial increase in internal loads to support external loads on the human spine [98]. Some studies have investigated the effects of muscle volume on the lumbar spinal column by including a passive muscle volume in the model [99, 100], while others have predicted muscle activation and spinal loads using the optimization method. Jamshidnejad and Arjmand [101] investigated the effects of paraspinal muscle intraoperative injuries on muscle activation and spinal loads and reported that trunk strength was reduced by 23% as a result of reductions in the cross-sectional area of the extensor muscles. El Ouaaid et al. [65] predicted trunk muscle forces using an FE model of the thoracolumbar spine with an optimization algorithm during lifting activities and noted that spinal force prediction was helpful to improve rehabilitation and stabilization exercise designs.

4 Conclusion

We reviewed the recent advances in FE modeling of the lumbar spine, including modeling and analysis from the bone to soft tissue and muscle forces, as well as the validation and application of these models. The discussion was associated with material properties, element types, loading and boundaries, and geometric parameters. In addition, muscle force modeling and the follower load concept were introduced. Furthermore, we summarized experimental ROM, FJF, and IDP data for validation of the lumbar spine FE model since all new models should be verified based on recognized intact models. Application studies were briefly reviewed, in which the majority of FE models focused on spinal degeneration diseases and surgical instrumentation techniques. Although muscle force prediction and optimization are challenging with FE modeling due to their complexity and redundancy, several studies have predicted muscle activation and spinal forces for injury prevention assessments and treatment strategies. The level of modeling prediction and representation can be improved with subject-specific data, and integration of FE and musculoskeletal models could generate a comprehensive analysis of the lumbar spine in clinical applications.

Acknowledgements This work was supported by Award number mfund-052022 from the Foundation for Science and Technology at Mongolian University of Science and Technology and the National Research Foundation of Korea (NRF) grants funded by the Korea government (MSIP) (NRF-2021R1A2C1011825).

Declarations

Conflict of interest The authors declare that there is no conflict of interest.

References

1. Kim, Y. H., Khuyagbaatar, B., & Kim, K. (2018). Recent advances in finite element modeling of the human cervical spine. *Journal of Mechanical Science and Technology*. https://doi.org/10.1007/s12206-017-1201-2
2. Affolter, C., Kedzierska, J., Vielma, T., Weisse, B., & Aiyangar, A. (2020). Estimating lumbar passive stiffness behaviour from subject-specific finite element models and in vivo 6DOF kinematics. *Journal of Biomechanics, 102*, 109681. https://doi.org/10.1016/j.jbiomech.2020.109681
3. Naserkhaki, S., Arjmand, N., Shirazi-Adl, A., Farahmand, F., & El-Rich, M. (2018). Effects of eight different ligament property datasets on biomechanics of a lumbar L4–L5 finite element model. *Journal of Biomechanics, 70*, 33–42. https://doi.org/10.1016/j.jbiomech.2017.05.003
4. Coombs, D. J., Rullkoetter, P. J., & Laz, P. J. (2017). Efficient probabilistic finite element analysis of a lumbar motion segment. *Journal of Biomechanics, 61*, 65–74. https://doi.org/10.1016/j.jbiomech.2017.07.002
5. Salvatore, G., Berton, A., Giambini, H., Ciuffreda, M., Florio, P., Longo, U. G., Denaro, V., Thoreson, A., & An, K. N. (2018). Biomechanical effects of metastasis in the osteoporotic lumbar spine: A finite element analysis. *BMC Musculoskeletal Disorders, 19*(1), 1–8. https://doi.org/10.1186/s12891-018-1953-6
6. Ambati, D. V., Wright, E. K., Lehman, R. A., Kang, D. G., Wagner, S. C., & Dmitriev, A. E. (2015). Bilateral pedicle screw fixation provides superior biomechanical stability in transforaminal lumbar interbody fusion: A finite element study. *Spine Journal, 15*(8), 1812–1822. https://doi.org/10.1016/j.spinee.2014.06.015
7. Xu, M., Yang, J., Lieberman, I., & Haddas, R. (2019). Stress distribution in vertebral bone and pedicle screw and screw–bone load transfers among various fixation methods for lumbar spine surgical alignment: A finite element study. *Medical Engineering and Physics, 63*, 26–32. https://doi.org/10.1016/j.medengphy.2018.10.003
8. Sterba, M., Aubin, C. É., Wagnac, E., Fradet, L., & Arnoux, P. J. (2019). Effect of impact velocity and ligament mechanical properties on lumbar spine injuries in posterior-anterior impact loading conditions: A finite element study. *Medical and Biological Engineering and Computing, 57*(6), 1381–1392. https://doi.org/10.1007/s11517-019-01964-5
9. Li, Q. Y., Kim, H. J., Son, J., Kang, K. T., Chang, B. S., Lee, C. K., Seok, H. S., & Yeom, J. S. (2017). Biomechanical analysis of lumbar decompression surgery in relation to degenerative changes in the lumbar spine: Validated finite element analysis. *Computers in Biology and Medicine, 89*(March), 512–519. https://doi.org/10.1016/j.compbiomed.2017.09.003
10. Wang, H., Wan, Y., Liu, X., Ren, B., Xia, Y., & Liu, Z. (2021). The biomechanical effects of Ti versus PEEK used in the PLIF surgery on lumbar spine: A finite element analysis. *Computer Methods in Biomechanics and Biomedical Engineering, 24*(10), 1115–1124. https://doi.org/10.1080/10255842.2020.1869219
11. Talukdar, R. G., Mukhopadhyay, K. K., Dhara, S., & Gupta, S. (2021). Numerical analysis of the mechanical behaviour of intact and implanted lumbar functional spinal units: Effects of loading and boundary conditions. *Proceedings of the Institution of Mechanical Engineers, Part H: Journal of Engineering in*

Medicine, 235(7), 792–804. https://doi.org/10.1177/09544119211008343
12. Shen, H., Chen, Y., Liao, Z., & Liu, W. (2021). Biomechanical evaluation of anterior lumbar interbody fusion with various fixation options: Finite element analysis of static and vibration conditions. *Clinical Biomechanics, 84*(March), 105339. https://doi.org/10.1016/j.clinbiomech.2021.105339
13. Guo, L. X., & Wang, Q. D. (2020). Biomechanical analysis of a new bilateral pedicle screw fixator system based on topological optimization. *International Journal of Precision Engineering and Manufacturing, 21*(7), 1363–1374. https://doi.org/10.1007/s12541-020-00336-6
14. Choi, J., Shin, D. A., & Kim, S. (2017). Biomechanical effects of the geometry of ball-and-socket artificial disc on lumbar spine. *Spine, 42*(6), E332–E339. https://doi.org/10.1097/BRS.0000000000001789
15. Guo, L. X., & Li, W. J. (2020). Finite element modeling and static/dynamic validation of thoracolumbar-pelvic segment. *Computer Methods in Biomechanics and Biomedical Engineering, 23*(2), 69–80. https://doi.org/10.1080/10255842.2019.1699543
16. Haddas, R., Xu, M., Lieberman, I., & Yang, J. (2019). Finite element based-analysis for pre and post lumbar fusion of adult degenerative scoliosis patients. *Spine Deformity, 7*(4), 543–552. https://doi.org/10.1016/j.jspd.2018.11.008
17. Haj-Ali, R., Wolfson, R., & Masharawi, Y. (2019). A patient specific computational biomechanical model for the entire lumbosacral spinal unit with imposed spondylolysis. *Clinical Biomechanics, 68*, 37–44. https://doi.org/10.1016/j.clinbiomech.2019.05.022
18. Joukar, A., Shah, A., Kiapour, A., Vosoughi, A. S., Duhon, B., Agarwal, A. K., Elgafy, H., Ebraheim, N., & Goel, V. K. (2018). Sex specific sacroiliac joint biomechanics during standing upright. *Spine, 43*(18), E1053–E1060. https://doi.org/10.1097/BRS.0000000000002623
19. Mills, M. J., & Sarigul-Klijn, N. (2019). Validation of an in vivo medical image-based young human lumbar spine finite element model. *Journal of Biomechanical Engineering*. https://doi.org/10.1115/1.4042183
20. Park, W. M., Kim, K., & Kim, Y. H. (2014). Biomechanical analysis of two-step traction therapy in the lumbar spine. *Manual Therapy, 19*(6), 527–533. https://doi.org/10.1016/j.math.2014.05.004
21. Zhang, H., & Zhu, W. (2019). The path to deliver the most realistic follower load for a lumbar spine in standing posture: A finite element study. *Journal of Biomechanical Engineering*. https://doi.org/10.1115/1.4042438
22. Park, W. M., Kim, K., & Kim, Y. H. (2013). Effects of degenerated intervertebral discs on intersegmental rotations, intradiscal pressures, and facet joint forces of the whole lumbar spine. *Computers in Biology and Medicine, 43*(9), 1234–1240. https://doi.org/10.1016/j.compbiomed.2013.06.011
23. Wang, Q. D., & Guo, L. X. (2021). Biomechanical role of nucleotomy in vibration characteristics of human spine. *International Journal of Precision Engineering and Manufacturing, 22*(7), 1323–1334. https://doi.org/10.1007/s12541-021-00519-9
24. Garavelli, C., Curreli, C., Palanca, M., Aldieri, A., Cristofolini, L., & Viceconti, M. (2022). Experimental validation of a subject-specific finite element model of lumbar spine segment using digital image correlation. *PLoS ONE, 17*(9), 1–17. https://doi.org/10.1371/journal.pone.0272529
25. Xu, M., Yang, J., Lieberman, I. H., & Haddas, R. (2017). Lumbar spine finite element model for healthy subjects: Development and validation. *Computer Methods in Biomechanics and Biomedical Engineering, 20*(1), 1–15. https://doi.org/10.1080/10255842.2016.1193596
26. Rayudu, N. M., Subburaj, K., Mohan, R. E., Sollmann, N., Dieckmeyer, M., Kirschke, J. S., & Baum, T. (2022). Patient-specific finite element modeling of the whole lumbar spine using clinical routine multi-detector computed tomography (MDCT) data: A pilot study. *Biomedicines*. https://doi.org/10.3390/biomedicines10071567
27. Khoddam-Khorasani, P., Arjmand, N., & Shirazi-Adl, A. (2018). Trunk hybrid passive-active musculoskeletal modeling to determine the detailed T12–S1 response under in vivo loads. *Annals of Biomedical Engineering, 46*(11), 1830–1843. https://doi.org/10.1007/s10439-018-2078-7
28. Rajaee, M. A., Arjmand, N., & Shirazi-Adl, A. (2021). A novel coupled musculoskeletal finite element model of the spine: Critical evaluation of trunk models in some tasks. *Journal of Biomechanics, 119*, 110331. https://doi.org/10.1016/j.jbiomech.2021.110331
29. Remus, R., Lipphaus, A., Neumann, M., & Bender, B. (2021). Calibration and validation of a novel hybrid model of the lumbosacral spine in ArtiSynth: The passive structures. *PLoS ONE*. https://doi.org/10.1371/journal.pone.0250456
30. Zhao, G., Wang, H., Wang, L., Ibrahim, Y., Wan, Y., Sun, J., Yuan, S., & Liu, X. (2022). The Biomechanical effects of different bag-carrying styles on lumbar spine and paraspinal muscles: A combined musculoskeletal and finite element study. *Orthopaedic Surgery, 15*, 315–327. https://doi.org/10.1111/os.13573
31. Kumaran, Y., Shah, A., Katragadda, A., Padgaonkar, A., Zavatsky, J., McGuire, R., Serhan, H., Elgafy, H., & Goel, V. K. (2021). Iatrogenic muscle damage in transforaminal lumbar interbody fusion and adjacent segment degeneration: A comparative finite element analysis of open and minimally invasive surgeries. *European Spine Journal, 30*(9), 2622–2630. https://doi.org/10.1007/s00586-021-06909-x
32. Liu, T., Khalaf, K., Adeeb, S., & El-Rich, M. (2019). Effects of lumbo-pelvic rhythm on trunk muscle forces and disc loads during forward flexion: A combined musculoskeletal and finite element simulation study. *Journal of Biomechanics, 82*, 116–123. https://doi.org/10.1016/j.jbiomech.2018.10.009
33. Honegger, J. D., Actis, J. A., Gates, D. H., Silverman, A. K., Munson, A. H., & Petrella, A. J. (2021). Development of a multiscale model of the human lumbar spine for investigation of tissue loads in people with and without a transtibial amputation during sit-to-stand. *Biomechanics and Modeling in Mechanobiology, 20*(1), 339–358. https://doi.org/10.1007/s10237-020-01389-2
34. Oxland, T. R. (2016). Fundamental biomechanics of the spine: What we have learned in the past 25 years and future directions. *Journal of Biomechanics, 49*(6), 817–832. https://doi.org/10.1016/j.jbiomech.2015.10.035
35. Freutel, M., Schmidt, H., Dürselen, L., Ignatius, A., & Galbusera, F. (2014). Finite element modeling of soft tissues: Material models, tissue interaction and challenges. *Clinical Biomechanics, 29*(4), 363–372. https://doi.org/10.1016/j.clinbiomech.2014.01.006
36. Schmidt, H., Galbusera, F., Rohlmann, A., & Shirazi-Adl, A. (2013). What have we learned from finite element model studies of lumbar intervertebral discs in the past four decades? *Journal of Biomechanics, 46*(14), 2342–2355. https://doi.org/10.1016/j.jbiomech.2013.07.014
37. Mengoni, M. (2021). Biomechanical modelling of the facet joints: A review of methods and validation processes in finite element analysis. *Biomechanics and Modeling in Mechanobiology, 20*(2), 389–401. https://doi.org/10.1007/s10237-020-01403-7
38. Ghezelbash, F., Schmidt, H., Shirazi-Adl, A., & El-Rich, M. (2020). Internal load-sharing in the human passive lumbar spine: Review of in vitro and finite element model studies. *Journal of Biomechanics, 102*, 109441. https://doi.org/10.1016/j.jbiomech.2019.109441

39. Jones, A. C., & Wilcox, R. K. (2008). Finite element analysis of the spine: Towards a framework of verification, validation and sensitivity analysis. *Medical Engineering and Physics, 30*(10), 1287–1304. https://doi.org/10.1016/j.medengphy.2008.09.006
40. Zhang, Q. H., & Teo, E. C. (2008). Finite element application in implant research for treatment of lumbar degenerative disc disease. *Medical Engineering and Physics, 30*(10), 1246–1256. https://doi.org/10.1016/j.medengphy.2008.07.012
41. Gould, S. L., Cristofolini, L., Davico, G., & Viceconti, M. (2021). Computational modelling of the scoliotic spine: A literature review. *International Journal for Numerical Methods in Biomedical Engineering, 37*(10), 1–27. https://doi.org/10.1002/cnm.3503
42. Alizadeh, M., Knapik, G. G., Mageswaran, P., Mendel, E., Bourekas, E., & Marras, W. S. (2020). Biomechanical musculoskeletal models of the cervical spine: A systematic literature review. *Clinical Biomechanics, 71*(April 2019), 115–124. https://doi.org/10.1016/j.clinbiomech.2019.10.027
43. Knapik, G. G., Mendel, E., Bourekas, E., & Marras, W. S. (2022). Computational lumbar spine models: A literature review. *Clinical Biomechanics, 100*, 105816. https://doi.org/10.1016/j.clinbiomech.2022.105816
44. Naoum, S., Vasiliadis, A. V., Koutserimpas, C., Mylonakis, N., Kotsapas, M., & Katakalos, K. (2021). Finite element method for the evaluation of the human spine: A literature overview. *Journal of Functional Biomaterials*. https://doi.org/10.3390/JFB12030043
45. Sciortino, V., Pasta, S., Ingrassia, T., & Cerniglia, D. (2023). On the finite element modeling of the lumbar spine: A schematic review. *Applied Sciences (Switzerland)*. https://doi.org/10.3390/app13020958
46. Dreischarf, M., Zander, T., Shirazi-Adl, A., Puttlitz, C. M., Adam, C. J., Chen, C. S., Goel, V. K., Kiapour, A., Kim, Y. H., Labus, K. M., Little, J. P., Park, W. M., Wang, Y. H., Wilke, H. J., Rohlmann, A., & Schmidt, H. (2014). Comparison of eight published static finite element models of the intact lumbar spine: Predictive power of models improves when combined together. *Journal of Biomechanics, 47*(8), 1757–1766. https://doi.org/10.1016/j.jbiomech.2014.04.002
47. Nikkhoo, M., Khoz, Z., Cheng, C. H., Niu, C. C., El-Rich, M., & Khalaf, K. (2020). Development of a novel geometrically-parametric patient-specific finite element model to investigate the effects of the lumbar lordosis angle on fusion surgery. *Journal of Biomechanics, 102*, 109722. https://doi.org/10.1016/j.jbiomech.2020.109722
48. Bashkuev, M., Reitmaier, S., & Schmidt, H. (2018). Effect of disc degeneration on the mechanical behavior of the human lumbar spine: A probabilistic finite element study. *Spine Journal, 18*(10), 1910–1920. https://doi.org/10.1016/j.spinee.2018.05.046
49. Campbell, J. Q., & Petrella, A. J. (2015). An automated method for landmark identification and finite-element modeling of the lumbar spine. *IEEE Transactions on Biomedical Engineering, 62*(11), 2709–2716. https://doi.org/10.1109/TBME.2015.2444811
50. Guldeniz, O., Yesil, O. B., & Okyar, F. (2022). Yeditepe spine mesh: Finite element modeling and validation of a parametric CAD model of lumbar spine. *Medical Engineering and Physics, 110*(August), 103911. https://doi.org/10.1016/j.medengphy.2022.103911
51. Umale, S., Yoganandan, N., & Kurpad, S. N. (2020). Development and validation of osteoligamentous lumbar spine under complex loading conditions: A step towards patient-specific modeling. *Journal of the Mechanical Behavior of Biomedical Materials, 110*(March), 103898. https://doi.org/10.1016/j.jmbbm.2020.103898
52. Lalonde, N. M., Petit, Y., Aubin, C. E., Wagnac, E., & Arnoux, P. J. (2013). Method to geometrically personalize a detailed finite-element model of the Spine. *IEEE Transactions on Biomedical Engineering, 60*(7), 2014–2021. https://doi.org/10.1109/TBME.2013.2246865
53. Zander, T., Dreischarf, M., Timm, A. K., Baumann, W. W., & Schmidt, H. (2017). Impact of material and morphological parameters on the mechanical response of the lumbar spine: A finite element sensitivity study. *Journal of Biomechanics, 53*, 185–190. https://doi.org/10.1016/j.jbiomech.2016.12.014
54. Ahuja, S., Moideen, A. N., Dudhniwala, A. G., Karatsis, E., Papadakis, L., & Varitis, E. (2020). Lumbar stability following graded unilateral and bilateral facetectomy: A finite element model study. *Clinical Biomechanics, 75*(July 2019), 105011. https://doi.org/10.1016/j.clinbiomech.2020.105011
55. Dreischarf, M., Rohlmann, A., Zhu, R., Schmidt, H., & Zander, T. (2013). Is it possible to estimate the compressive force in the lumbar spine from intradiscal pressure measurements? A finite element evaluation. *Medical Engineering and Physics, 35*(9), 1385–1390. https://doi.org/10.1016/j.medengphy.2013.03.007
56. Fan, W., & Guo, L. X. (2018). Finite element investigation of the effect of nucleus removal on vibration characteristics of the lumbar spine under a compressive follower preload. *Journal of the Mechanical Behavior of Biomedical Materials, 78*(3), 342–351. https://doi.org/10.1016/j.jmbbm.2017.11.040
57. Leszczynski, A., Meyer, F., Charles, Y. P., Deck, C., & Willinger, R. (2022). Development of a flexible instrumented lumbar spine finite element model and comparison with in-vitro experiments. *Computer Methods in Biomechanics and Biomedical Engineering, 25*(2), 221–237. https://doi.org/10.1080/10255842.2021.1948021
58. Wang, K., Jiang, C., Wang, L., Wang, H., & Niu, W. (2018). The biomechanical influence of anterior vertebral body osteophytes on the lumbar spine: A finite element study. *Spine Journal, 18*(12), 2288–2296. https://doi.org/10.1016/j.spinee.2018.07.001
59. Rohlmann, A., Burra, N. K., Zander, T., & Bergmann, G. (2007). Comparison of the effects of bilateral posterior dynamic and rigid fixation devices on the loads in the lumbar spine: A finite element analysis. *European Spine Journal, 16*(8), 1223–1231. https://doi.org/10.1007/s00586-006-0292-8
60. Park, W. M., Choi, D. K., Kim, K., Kim, Y. J., & Kim, Y. H. (2015). Biomechanical effects of fusion levels on the risk of proximal junctional failure and kyphosis in lumbar spinal fusion surgery. *Clinical Biomechanics, 30*(10), 1162–1169. https://doi.org/10.1016/j.clinbiomech.2015.08.009
61. Naserkhaki, S., & El-Rich, M. (2017). Sensitivity of lumbar spine response to follower load and flexion moment: Finite element study. *Computer Methods in Biomechanics and Biomedical Engineering, 20*(5), 550–557. https://doi.org/10.1080/10255842.2016.1257707
62. Spina, N. T., Moreno, G. S., Brodke, D. S., Finley, S. M., & Ellis, B. J. (2021). Biomechanical effects of laminectomies in the human lumbar spine: A finite element study. *Spine Journal, 21*(1), 150–159. https://doi.org/10.1016/j.spinee.2020.07.016
63. Kim, K., Kim, Y. H., & Lee, S. K. (2007). Increase of load-carrying capacity under follower load generated by trunk muscles in lumbar spine. *Proceedings of the Institution of Mechanical Engineers, Part H: Journal of Engineering in Medicine, 221*(3), 229–235. https://doi.org/10.1243/09544119JEIM229
64. Kim, K., & Kim, Y. H. (2008). Role of trunk muscles in generating follower load in the lumbar spine of neutral standing posture. *Journal of Biomechanical Engineering*. https://doi.org/10.1115/1.2907739

65. Ouaaid, Z. E., Arjmand, N., Shirazi-Adl, A., & Parnianpour, M. (2009). A novel approach to evaluate abdominal coactivities for optimal spinal stability and compression force in lifting. *Computer Methods in Biomechanics and Biomedical Engineering, 12*(6), 735–745. https://doi.org/10.1080/10255840902896018
66. El Ouaaid, Z., Shirazi-Adl, A., & Plamondon, A. (2018). Trunk response and stability in standing under sagittal-symmetric pull–push forces at different orientations, elevations and magnitudes. *Journal of Biomechanics, 70*, 166–174. https://doi.org/10.1016/j.jbiomech.2017.10.008
67. Guan, Y., Yoganandan, N., Moore, J., Pintar, F. A., Zhang, J., Maiman, D. J., & Laud, P. (2007). Moment-rotation responses of the human lumbosacral spinal column. *Journal of Biomechanics, 40*(9), 1975–1980. https://doi.org/10.1016/j.jbiomech.2006.09.027
68. Rohlmann, A., Zander, T., Rao, M., & Bergmann, G. (2009). Applying a follower load delivers realistic results for simulating standing. *Journal of Biomechanics, 42*(10), 1520–1526. https://doi.org/10.1016/j.jbiomech.2009.03.048
69. Han, K. S., Rohlmann, A., Yang, S. J., Kim, B. S., & Lim, T. H. (2011). Spinal muscles can create compressive follower loads in the lumbar spine in a neutral standing posture. *Medical Engineering and Physics, 33*(4), 472–478. https://doi.org/10.1016/j.medengphy.2010.11.014
70. Shih, K. S., Weng, P. W., Lin, S. C., Chen, Y. T., Cheng, C. K., & Lee, C. H. (2016). Biomechanical comparison between concentrated, follower, and muscular loads of the lumbar column. *Computer Methods and Programs in Biomedicine, 135*, 209–218. https://doi.org/10.1016/j.cmpb.2016.07.021
71. Azadi, A., & Arjmand, N. (2021). A comprehensive approach for the validation of lumbar spine finite element models investigating post-fusion adjacent segment effects. *Journal of Biomechanics, 121*, 110430. https://doi.org/10.1016/j.jbiomech.2021.110430
72. Rohlmann, A., Neller, S., Claes, L., Bergmann, G., & Wilke, H. J. (2001). Influence of a follower load on intradiscal pressure and intersegmental rotation of the lumbar spine. *Spine, 26*(24), 557–561. https://doi.org/10.1097/00007632-200112150-00014
73. Shirazi-Adl, A. (1994). Nonlinear stress analysis of the whole lumbar spine in torsion-Mechanics of facet articulation. *Journal of Biomechanics*. https://doi.org/10.1016/0021-9290(94)90005-1
74. Sawa, A. G. U., & Crawford, N. R. (2008). The use of surface strain data and a neural networks solution method to determine lumbar facet joint loads during in vitro spine testing. *Journal of Biomechanics, 41*(12), 2647–2653. https://doi.org/10.1016/j.jbiomech.2008.06.010
75. Wilson, D. C., Niosi, C. A., Zhu, Q. A., Oxland, T. R., & Wilson, D. R. (2006). Accuracy and repeatability of a new method for measuring facet loads in the lumbar spine. *Journal of Biomechanics, 39*(2), 348–353. https://doi.org/10.1016/j.jbiomech.2004.12.011
76. Zhu, Q. A., Park, Y. B., Sjovold, S. G., Niosi, C. A., Wilson, D. C., Cripton, P. A., & Oxland, T. R. (2008). Can extra-articular strains be used to measure facet contact forces in the lumbar spine? An in-vitro biomechanical study. *Proceedings of the Institution of Mechanical Engineers, Part H: Journal of Engineering in Medicine, 222*(2), 171–184. https://doi.org/10.1243/09544119JEIM290
77. Brinckmann, P., & Grootenboer, H. (1991). Change of disc height, radial disc bulge, and intradiscal pressure from discectomy: An in vitro investigation on human lumbar discs. *Spine, 16*(6), 641–646. https://doi.org/10.1097/00007632-199106000-00008
78. Wilke, H. J., Neef, P., Hinz, B., Seidel, H., & Claes, L. (2001). Intradiscal pressure together with anthropometric data: A data set for the validation of models. *Clinical Biomechanics*. https://doi.org/10.1016/s0268-0033(00)00103-0
79. Ellingson, A. M., Shaw, M. N., Giambini, H., & An, K.-N. (2016). Comparative role of disc degeneration and ligament failure on functional mechanics of the lumbar spine. *Computer Methods in Biomechanics and Biomedical Engineering, 19*(9), 1009–1018. https://doi.org/10.1080/10255842.2015.1088524
80. Natarajan, R. N., Williams, J. R., & Andersson, G. B. J. (2004). Recent advances in analytical modeling of lumbar disc degeneration. *Spine, 29*(23), 2733–2741. https://doi.org/10.1097/01.brs.0000146471.59052.e6
81. Rohlmann, A., Zander, T., Schmidt, H., Wilke, H. J., & Bergmann, G. (2006). Analysis of the influence of disc degeneration on the mechanical behaviour of a lumbar motion segment using the finite element method. *Journal of Biomechanics, 39*(13), 2484–2490. https://doi.org/10.1016/j.jbiomech.2005.07.026
82. Kang, S., Park, C. H., Jung, H., Lee, S., Min, Y. S., Kim, C. H., Cho, M., Jung, G. H., Kim, D. H., Kim, K. T., & Hwang, J. M. (2022). Analysis of the physiological load on lumbar vertebrae in patients with osteoporosis: A finite-element study. *Scientific Reports, 12*(1), 1–14. https://doi.org/10.1038/s41598-022-15241-3
83. Natarajan, R. N., Watanabe, K., & Hasegawa, K. (2020). Posterior bone graft in lumbar spine surgery reduces the stress in the screw-rod system: A finite element study. *Journal of the Mechanical Behavior of Biomedical Materials, 104*(December 2019), 103628. https://doi.org/10.1016/j.jmbbm.2020.103628
84. Wang, Q. D., & Guo, L. X. (2021). Prediction of complications and fusion outcomes of fused lumbar spine with or without fixation system under whole-body vibration. *Medical and Biological Engineering and Computing, 59*(6), 1223–1233. https://doi.org/10.1007/s11517-021-02375-1
85. Biswas, J. K., Rana, M., Majumder, S., Karmakar, S. K., & Roychowdhury, A. (2018). Effect of two-level pedicle-screw fixation with different rod materials on lumbar spine: A finite element study. *Journal of Orthopaedic Science, 23*(2), 258–265. https://doi.org/10.1016/j.jos.2017.10.009
86. Chen, C. S., Huang, C. H., & Shih, S. L. (2015). Biomechanical evaluation of a new pedicle screw-based posterior dynamic stabilization device (Awesome Rod System): A finite element analysis. *BMC Musculoskeletal Disorders, 16*(1), 1–8. https://doi.org/10.1186/s12891-015-0538-x
87. Choi, H. W., Kim, Y. E., & Chae, S. W. (2016). Effects of the level of mono-segmental dynamic stabilization on the whole lumbar spine. *International Journal of Precision Engineering and Manufacturing, 17*(5), 603–611. https://doi.org/10.1007/s12541-016-0073-1
88. Oktenoglu, T., Erbulut, D. U., Kiapour, A., Ozer, A. F., Lazoglu, I., Kaner, T., Sasani, M., & Goel, V. K. (2015). Pedicle screw-based posterior dynamic stabilisation of the lumbar spine: In vitro cadaver investigation and a finite element study. *Computer Methods in Biomechanics and Biomedical Engineering, 18*(11), 1252–1261. https://doi.org/10.1080/10255842.2014.890187
89. Heo, M., Yun, J., Kim, H., Lee, S. S., & Park, S. (2022). Optimization of a lumbar interspinous fixation device for the lumbar spine with degenerative disc disease. *PLoS ONE, 17*(4 April), 1–18. https://doi.org/10.1371/journal.pone.0265926
90. Más, Y., Gracia, L., Ibarz, E., Gabarre, S., Peña, D., & Herrera, A. (2017). Finite element simulation and clinical followup of lumbar spine biomechanics with dynamic fixations. *PLoS ONE*. https://doi.org/10.1371/journal.pone.0188328
91. Jia, H., Xu, B., & Qi, X. (2022). Biomechanical evaluation of percutaneous cement discoplasty by finite element analysis. *BMC Musculoskeletal Disorders, 23*(1), 1–12. https://doi.org/10.1186/s12891-022-05508-1
92. Kim, H. J., Chun, H. J., Kang, K. T., Lee, H. M., Chang, B. S., Lee, C. K., & Yeom, J. S. (2015). Finite element analysis

for comparison of spinous process osteotomies technique with conventional laminectomy as lumbar decompression procedure. *Yonsei Medical Journal, 56*(1), 146–153. https://doi.org/10.3349/ymj.2015.56.1.146

93. Ottardi, C., Galbusera, F., Luca, A., Prosdocimo, L., Sasso, M., Brayda-Bruno, M., & Villa, T. (2016). Finite element analysis of the lumbar destabilization following pedicle subtraction osteotomy. *Medical Engineering and Physics, 38*(5), 506–509. https://doi.org/10.1016/j.medengphy.2016.02.002
94. Zhang, Q., Chon, T. E., Zhang, Y., Baker, J. S., & Gu, Y. (2021). Finite element analysis of the lumbar spine in adolescent idiopathic scoliosis subjected to different loads. *Computers in Biology and Medicine, 136*(818), 104745. https://doi.org/10.1016/j.compbiomed.2021.104745
95. Che, M., Wang, Y., Zhao, Y., Zhang, S., Yu, J., Gong, W., Zhang, D., & Liu, M. (2022). Finite element analysis of a new type of spinal protection device for the prevention and treatment of osteoporotic vertebral compression fractures. *Orthopaedic Surgery, 14*(3), 577–586. https://doi.org/10.1111/os.13220
96. Kim, Y. H., Kim, K., & Park, W. M. (2021). Biomechanical influence of treatment table axis location on axial rotation of lumbar spine. *International Journal of Precision Engineering and Manufacturing, 22*(5), 889–897. https://doi.org/10.1007/s12541-021-00499-w
97. Fan, W., & Guo, L. X. (2017). Influence of different frequencies of axial cyclic loading on time-domain vibration response of the lumbar spine: A finite element study. *Computers in Biology and Medicine, 86*(3), 75–81. https://doi.org/10.1016/j.compbiomed.2017.05.004
98. Dreischarf, M., Shirazi-Adl, A., Arjmand, N., Rohlmann, A., & Schmidt, H. (2016). Estimation of loads on human lumbar spine: A review of in vivo and computational model studies. *Journal of Biomechanics, 49*(6), 833–845. https://doi.org/10.1016/j.jbiomech.2015.12.038
99. Kang, I., Choi, M., Lee, D., & Noh, G. (2020). Effect of passive support of the spinal muscles on the biomechanics of a lumbar finite element model. *Applied Sciences (Switzerland)*. https://doi.org/10.3390/APP10186278
100. Kang, S., Chang, M. C., Kim, H., Kim, J., Jang, Y., Park, D., & Hwang, J. M. (2021). The effects of paraspinal muscle volume on physiological load on the lumbar vertebral column: A finite-element study. *Spine, 46*(19), E1015–E1021. https://doi.org/10.1097/BRS.0000000000004014
101. Jamshidnejad, S., & Arjmand, N. (2015). Variations in trunk muscle activities and spinal loads following posterior lumbar surgery: A combined in vivo and modeling investigation. *Clinical Biomechanics, 30*(10), 1036–1042. https://doi.org/10.1016/j.clinbiomech.2015.09.010

Batbayar Khuyagbaatar received his B.S. and M.S. from Mongolian University of Science and Technology in 2008 and 2010, respectively, and Ph.D. in mechanical engineering from Kyung Hee University in 2016. He is a professor in the Department of Technical Mechanics, Mongolian University of Science and Technology, Mongolia.

Kyungsoo Kim received his B.S., M.S., and Ph.D. in mathematics from Korea Advanced Institute of Science and Technology (KAIST) in 1996, 1998, and 2003, respectively. He is a professor in the Department of Applied Mathematics, Kyung Hee University, Korea.

Yoon Hyuk Kim received his B.S., M.S. and Ph.D. in mechanical engineering from Korea Advanced Institute of Science and Technology (KAIST) in 1992, 1994, and 2000, respectively. He is a professor in the Department of Mechanical Engineering, Kyung Hee University, Korea.